

Figure 4 Measured 90° and 180° phase shifting. [Color figure can be viewed in the online issue, which is available at wileyonlinelibrary.com]

spectrum of the generated CS signal, the optical spectrum presents two phase-locked carriers, which are 26.75 GHz apart. Curves B and C are the spectrums of the two demultiplexed phase-locked carriers and curve D is the spectrum of the phase shifted CS signal.

The phase shifting performance of the proposed photonic RF phase shifter was measured by rotating the WP in a HQQ type PC. As shown in Figure 3, a rotation angle of PC that ranges from -50° to $+50^\circ$ can induce a near-linear phase shifting exceeding 360° and a phase shifting higher than 180° is expected if the rotation angle of PC is increased further. Figure 4 illustrates that the linear RF phase shifter induces a 9.3 ps and 18.7 ps delay (i.e., a 90° and 180° phase shifting) compared with the input RF signal when the rotation angle of PC is set at 22.5° and 45° , respectively.

5. CONCLUSIONS

In this article, a RF photonic phase shifter based on PC is realized and the theoretical fundamentals of this scheme are analyzed. A prototype with 26.75 GHz bandwidth is experimentally demonstrated and a near-linear 360° phase shift tuning range is achieved.

ACKNOWLEDGMENTS

This work is supported by the National Natural Science Foundation of China (Grant No. 60932003) and the National High-tech R&D Program of China (863 Program, Grant No. 2007AA01Z452 and 2009AA01Z118).

REFERENCES

1. M.L. VanBlaricum, Photonic systems for antenna applications, *IEEE Antennas Propag Mag* 36 (1994), 30–38.
2. J.J. Lee, R.Y. Loo, S. Livingston, V.I. Jones, J.B. Lewis, H.W. Yen, G.L. Tangonan, and M. Wechsberg, Photonic wideband array antennas, *IEEE Trans Antennas Propag* 43 (1995), 966–982.
3. M.R. Fisher and S.L. Chuang, A microwave photonic phase-shifter based on wavelength conversion in a DFB laser, *IEEE Photonics Technol Lett* 18 (2006), 1714–1716.
4. J. Han, H. Erlig, D. Chang, M.C. Oh, H. Zhang, C. Zhang, W. Steier, and H. Fetterman, Multiple output photonic RF phase shifter using a novel polymer technology, *IEEE Photonics Technol Lett* 14 (2002), 531–533.
5. S.S. Lee, A.H. Udupa, H. Erlig, H. Zhang, Y. Chang, C. Zhang, D.H. Chang, D. Bhattacharya, B. Tsap, W.H. Steier, L.R. Dalton, and H.R. Fetterman, Demonstration of a photonic controlled RF phase shifter, *IEEE Microwave Guided Wave Lett* 9 (1999), 357–359.
6. S.T. Winnall, A.C. Lindsay, and G.A. Knight, A wide-band microwave photonic phase and frequency shifter, *IEEE Trans Microwave Theory Tech* 45 (1997), 1003–1006.
7. J.F. Coward, T.K. Yee, C.H. Chalfant, and P.H. Chang, A photonic integrated-optic RF phase shifter for phased array antenna beam-forming applications, *J Lightwave Technol* 11 (1993), 2201–2205.
8. A. Loayssa and F.J. Lahoz, Broad-band RF photonic phase shifter based on stimulated Brillouin scattering and single-sideband modulation, *IEEE Photonics Technol Lett* 18 (2006), 208–210.
9. Y. Dong, H. He, W. Hu, Z. Li, Q. Wang, W. Kuang, T.H. Cheng, Y.J. Wen, Y. Wang, and C. Lu, Photonic microwave phase shifter/modulator based on a nonlinear optical loop mirror incorporating a Mach-Zehnder interferometer, *Opt Lett* 32 (2007), 745–747.
10. L. Goldberg, H.F. Taylor, J.F. Weller, and D.M. Bloom, Microwave signal generation with injection-locked laser diodes, *Electron Lett* 19 (1983), 491–493.
11. H.R. Rideout, J.S. Seregelyi, S. Paquet, and J. Yao, Discriminator-aided optical phase-lock loop incorporating a frequency down-conversion module, *IEEE Photonics Technol Lett* 18 (2006), 2344–2346.
12. X. Chen, Z. Deng, and J. Yao, Photonic generation of microwave signal using a dual-wavelength single-longitudinal-mode fiber ring laser, *IEEE Trans Microwave Theory Tech* 54 (2006), 804–809.
13. J.J. O'reilly, P.M. Lane, R. Heidemann, and R. Hofstetter, Optical generation of very narrow linewidth millimeter wave signals, *Electron Lett* 28 (1992), 2309–2311.
14. P.J. Winzer and R.J. Essiambre, Advanced modulation formats for high-capacity optical transport networks, *J Lightwave Technol* 24 (2006), 4711–4728.

© 2010 Wiley Periodicals, Inc.

NOISE-PARAMETER MEASUREMENTS WITH A REFLECTION TYPE PHASE SHIFTER*

Dazhen Gu,¹ David K. Walter,¹ and James Randa^{1,2}

¹Electromagnetics Division, National Institute of Standards and Technology, 325 Broadway, Boulder, CO 80305; Corresponding author: dazhen.gu@boulder.nist.gov

²Department of Physics, University of Colorado, Boulder, CO 80309

Received 8 February 2010

ABSTRACT: We report a miniaturized phase shifter operating in the frequency range from 5 to 7 GHz for noise-parameter extraction. Such a tunable solid-state unit represents a significant reduction in the size and

*This is a U.S. government work, but not protected by U.S. copyright.

mass as a source-pull component, compared to its mechanical counterparts. It provides adequate impedance coverage, ultra-fast response, as well as high repeatability, across the designed region. A packaged low-noise amplifier was measured at integer frequencies by use of the phase shifter on the NIST NFRad system. The measured results exhibited good accuracy. The combined uncertainties (Type-A and Type-B) are below 6% for both the minimum noise temperature and the magnitude of the optimum input reflection coefficient. © 2010 Wiley Periodicals, Inc. Microwave Opt Technol Lett 52:2600–2603, 2010; View this article online at wileyonlinelibrary.com. DOI 10.1002/mop.25532

Key words: amplifier noise parameters; noise measurement; phase shifter; source pull technique; uncertainty analysis

1. INTRODUCTION

Noise-parameter measurements generally require the presence of multiple impedance states at the input of a low-noise amplifier (LNA) to produce an overdetermination for solving four unknown scalars: minimum noise temperature T_{\min} , noise resistance R_n , and optimal complex reflection coefficient of the source Γ_{opt} .

The traditional source-pull bench usually employs a mechanical tuner system. It can provide excellent mapping on the Smith chart; however, its repeatability is questionable [1]. A solid-state tuner has a much smaller footprint when compared to its mechanical counterpart. It is often composed of two identical arrays of n PIN diodes toggled between fully on/off conditions to produce $(n + 1)^2$ impedance states [1]. Its discrete impedance states can provide an adequate coverage on the Smith chart. Also, a solid-state tuner has a high-power handling capability, making it capable of both source-pulling and load-pulling. Most recently, the National Institute of Standards and Technology (NIST) has developed a 1–12 GHz variable termination unit (VTU), consisting of electromechanical switches terminated with various reflective devices and noise diodes [2]. Such a unit provides a variety of impedance and noise-temperature states and has demonstrated improved time efficiency and satisfactory accuracy in noise-parameter measurements. However the VTU does have limitations. For example, it somewhat lacks portability. The VTU requires a configured switch controller and possesses a big footprint and large mass. In addition, mounting the VTU to the front-end noise temperature measurement system requires a great effort for achieving a stressless connection.

In this article, we present a solid-state phase shifter based on varactors operating between 5 and 7 GHz. The development of such a component will in particular benefit the metrology of LNAs in the wireless local area network (WLAN) band, such as IEEE 802.11a in the US and HiperLAN/2 in Europe with a bandwidth of 5.15–5.825 GHz.

2. DESIGN AND FABRICATION OF THE PHASE SHIFTER

A reflection type phase shifter consists of a 90° hybrid with its through port and its coupling port terminated by tunable delay lines or variable reactance. We selected the branch-line coupler to form the 90° hybrid because it is easy to design and fabricate. To achieve compactness, we use surface mountable varactors as variable reactance devices. A schematic of the phase shifter is illustrated in Figure 1(a).

We set the isolation port of the coupler to be open and make it a one-port device, a different configuration from conventional two-port phase shifters. For the source-pull purpose, we need to provide a number of states presented at the input of the amplifier. As we have discussed in the previous report [2], the use of highly reflective states (large $|\Gamma|$) leads to the minimum mea-

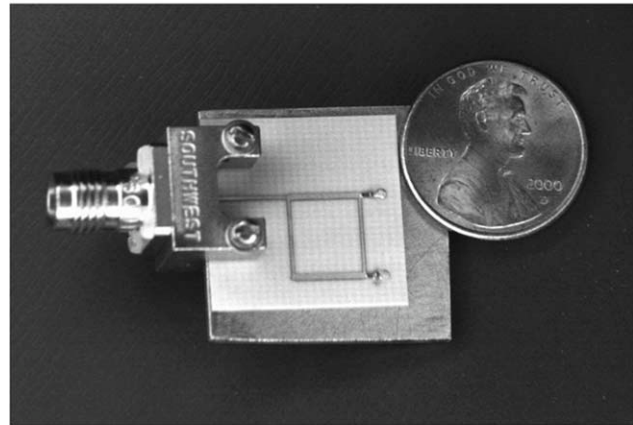
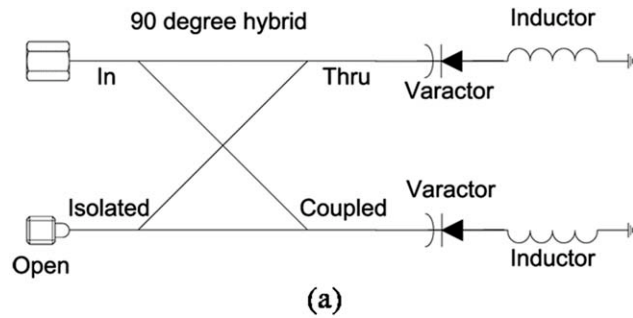


Figure 1 (a) Schematic of reflection phase shifter with two arms terminated with LC loads for improved tunability. (b) A photograph of the fabricated phase shifter

surement uncertainties for characterization of packaged LNAs. Therefore, an open termination introduced at the output of the phase shifter will result in a large reflection with a series of electrical delays seen at the reference plane of the input, which in turn diminish the error of noise-parameter measurements.

A coverage of four quadrants on the Smith chart is desirable to offer enough redundancy for noise-parameter fitting. A 180° phase shifter provides a 360° phase difference, given that the output is terminated with an open load. The maximum phase shift is 83° at 6 GHz with a capacitance change from 0.2 pF to 1 pF provided by varactors. An addition of a 1.6 nH inductor immediately following each varactor increases the phase shift capability to 179° between the input and the output, which satisfies the design criteria. The optimized value of the inductor is determined in the final circuit simulation.

The branch-line coupler was designed for a center frequency of 6 GHz on a 203 μm thick printed circuit board (PCB) with a relative dielectric constant of 3.55. The branch was composed of quarter-wavelength long transmission lines with impedances of Z_0 and $Z_0/\sqrt{2}$, representing a simple and compact design at the price of a limited bandwidth. An electromagnetic (EM) simulator was then used to optimize the dimensions. Simulated data show a return loss of 36 dB, an isolation of 32 dB, and a coupling factor of about 3 dB at 6 GHz for the optimized 90° hybrid. The via-holes needed for DC bias on the varactors were also simulated in the EM software, and the result was fitted to an equivalence of a 0.1 nH inductor.

A circuit model associated with the varactor diodes and predetermined values of other components were used in a microwave simulator to finalize the inductor value to be used in the circuit. An inductor of 1.0 nH proved adequate for achieving a good mapping on the Smith chart.

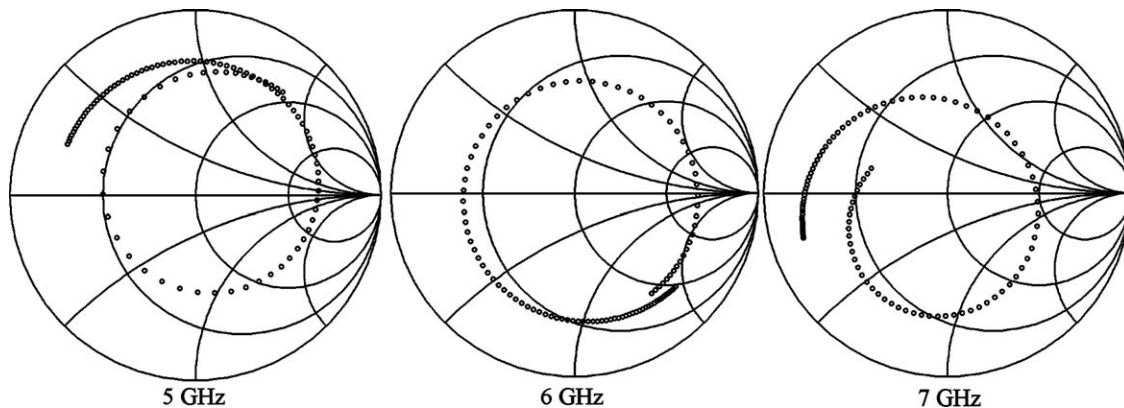


Figure 2 Measured impedance coverage at 5 GHz, 6 GHz, and 7 GHz shows sufficient tuning range

The PCB was patterned by use of photo-lithography and copper etching processes. The varactors and chip inductors were glued onto the board with silver epoxy and then cured at 150°C. The output of the coupler was left unterminated as an open. A photograph of the component is shown in Figure 1(b). The phase shifter has a dimension of about 3 cm by 5 cm and a weight of 19 g, including the connector and a copper shim for improving rigidity. The substantially reduced size and mass (more than 50 times) of the phase shifter represents a major advantage over the mechanical tuner and the VTU.

3. CHARACTERIZATION OF PHASE SHIFTER

The phase shifter was characterized on a vector network analyzer (VNA) in the frequency range of 4–8 GHz. The VNA was calibrated by use of a 1-port short-open-load (SOL) method. An external bias-tee was used to supply the DC bias to the varactor in the range of 0–10 V. The current drawn by the varactors is below the limit of the current meter (1 μ A) during operation, which agreed well with the circuit model (maximum 200 nA below 10 V).

The DC bias was cycled 10 times by 0.1 V per step between 0 and 10 V. Reflection coefficients were measured at each bias point on the VNA and the repeatability was checked. We observed a maximum standard deviation of about 0.0005, an indication of excellent repeatability. The standard deviation is well below the repeatability error of the 7-mm connector (~ 0.001), which covers the negligible error from the phase shifter. We note that no temperature regulation was necessary because the diodes dissipated an insignificant amount of power, so that the temperature of the entire unit remained at ambient within the uncertainty. Moreover, the varactor responded at a time scale of picoseconds, much faster than the electro-mechanical switch in the VTU and the movable slug in the mechanical tuner.

Figure 2 presents the measured reflection coefficients at 5 GHz, 6 GHz, and 7 GHz. The measured phase tuning capability is greater than 360° at frequencies between 5 and 7 GHz. At frequencies different from the design frequency (6 GHz), the magnitude of the reflection coefficient becomes less consistent across the tunable range. Such degraded functionality is primarily due to the narrow band characteristics of the branch-line coupler. Furthermore, the magnitude of the reflection coefficient is smaller than 1, mainly due to the coaxial-to-microstrip transition loss (~ 0.6 dB from a separate study), as well as the finite quality factor of the surface mountable components. Nonetheless, these discrepancies from the ideal design would not considerably limit the ability of the unit used for noise-parameter measurements.

A total of 9 bias voltages were chosen to produce 9 impedance states at each frequency point (5 GHz, 6 GHz, and 7

GHz). These states were scattered over the four quadrants of the Smith chart and were well suited for the source-pull measurements on a packaged amplifier.

4. NOISE-PARAMETER MEASUREMENT

Our noise-parameter measurement relies on the NIST NFRad system and the measurement setup has been discussed in detail elsewhere [3]. Figure 3 shows a schematic of noise-parameter measurements on a packaged LNA with the phase shifter. Prior to the noise-parameter measurement, reflection coefficients at plane 1, plane 2, and plane 2' for each bias point of the phase shifter were measured on the VNA, and all the data were transferred to the PC that controlled the NFRad. The input noise temperatures at plane 1 for all the impedance states were measured first. Next, the output noise temperature at plane 2' was read forty times consecutively. The effective noise temperature at plane 2 was corrected from plane 2' by the efficiency of the attenuator. A noise diode was used as an additional input termination to give a well matched and much warmer source as compared to the phase shifter. This allowed us to get more diversity of the impedance and obtain the amplifier gain from the noise-parameter fitting. Also, a reverse configured LNA was measured on the NFRad as a direct check of the noise emission from the input of the LNA [4].

The general theoretical framework of the noise-parameter fit is outlined in Ref. 5. Basically, the wave representation variables (X parameters) were first resolved in the data fitting and then translated to the IEEE parameters. The reduced gain, defined by $G_0 \equiv |S_{21}|^2$, where S_{21} is the transmission S -parameter of the LNA, can also be obtained from the fitting.

Fitted results of the LNA at integer frequencies are shown in Figure 4. The error bars indicate the overall standard deviation, a combination of type-A and type-B uncertainties. Type-A uncertainty is the direct outcome from the least-square fitting

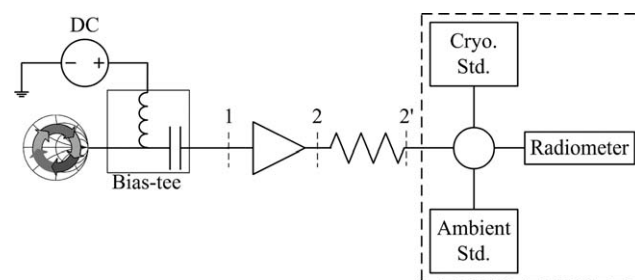


Figure 3 Illustration of the noise-temperature measurement setup. The components in the dashed box represent part of the NIST NFRad system

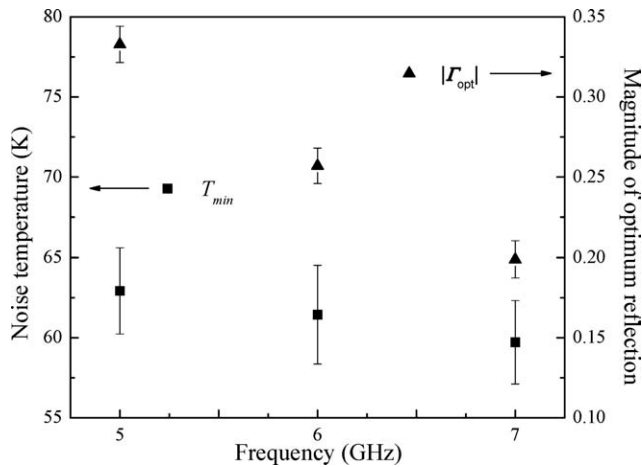


Figure 4 Fitted results of LNA T_{min} and LNA $|\Gamma_{opt}|$ from five day VTU measurements. Error bars indicate the standard uncertainty (1σ)

program. Type-B uncertainty is evaluated through a Monte Carlo simulation program [5]. The uncertainties in T_{min} at all frequencies are below 5.1%, and the uncertainties in $|\Gamma_{opt}|$ are below 5.8%. The fitted reduced gain is within 0.065 dB difference from the values measured on the VNA (~ 32.4 dB) at all three frequency points. These results are comparable to the previous VTU measurements [2].

5. DISCUSSION AND CONCLUSIONS

Here, we want to emphasize that we have not exercised intensive efforts in the design of a high-end component. Rather, the goal of this article is to demonstrate, for the first time, an efficient noise-parameter de-embedding method by use of a simplified phase shifter. In comparison to commercially available solid-state tuners based on PIN-diode arrays, the phase shifter consisting of varactors is a continuous impedance synthesizer, requiring fewer numbers of components to provide the same number of impedance states. Furthermore, PIN-diodes at fully on state draw non-negligible currents and contribute shot noise in addition to thermal noise [6]. For precision measurement purpose, they can be no longer considered as passive devices and need extra step to characterize their noise emission.

However, the prototype phase shifter used for noise-parameter measurements does need improvements. It has limited bandwidth and its reflection magnitude is not variable. First, a broadband coupler can be designed by means of a multi-layer microstrip circuit [7], although that increases the complexity in fabrication and packaging. Second, the reflection magnitude can be increased by improving the microstrip-to-coaxial coupling. Moreover, the parasitic resistance of the varactor can be compensated by adding a bipolar junction transistor (BJT) in series, which has negative resistance characteristic [8]. Third, rather than leaving it unconnected, we can terminate the isolation port of the coupler with a junction field-effect transistor (JFET), functioning as a voltage controlled resistor (VCR). Therefore, the magnitude of the reflection will be also adjustable, which in turn creates more mapping capability on the Smith chart.

In conclusion, we have successfully demonstrated the design, fabrication, and implementation of a 5–7 GHz phase shifter for noise-parameter extraction on a packaged amplifier. The phase shifter provides ultra-portability and fast response, far better than a mechanical tuner. Its good repeatability ensures the direct use on noise temperature instruments without online VNA requirement. The measured results showed acceptable uncer-

tainty. We also expect that the design is compatible with the transistor fabrication process and can potentially be incorporated onto the same wafer to provide quick on-wafer metrology.

REFERENCES

1. C.E. Woodin and D.L. Wandrei, High power solid state programmable load, U.S. Patent 5,276,411 (1994).
2. D. Gu, D.K. Walker, and J. Randa, Variable termination unit for noise parameter measurement, IEEE Trans Instrum Meas 58 (2008), 1072–1077.
3. C.A. Grosvenor, J. Randa, and R.L. Billinger, Design and testing of NFRad—A new noise measurement system, NIST Technical Note, TN1518, NIST, Boulder, CO (2000).
4. J. Randa and D.K. Walker, Amplifier noise-parameter measurement checks and verification, Presented at the 63rd ARFTG Conference Digest, Fort Worth, TX (2004), pp. 41–45.
5. J. Randa, Uncertainty analysis for noise-parameter measurements at NIST, IEEE Trans Instrum Meas 58 (2009) 1146–1151.
6. M. Jankovec, H. Stiebig, F. Smole, and M. Topic, Noise characterization of a-Si:H pin diodes, J Non Cryst Solids 352 (2006), 1829–1831.
7. A.M. Abbosh and M.E. Bialkowski, Design of compact directional couplers for UWB applications, IEEE Trans Microwave Theory Tech 55 (2007), 189–194.
8. K.T. Park, Y.H. Cho, and S.W. Yun, Low voltage tunable narrow bandpass filter using cross-coupled stepped-impedance resonator with active capacitance circuit, IEEE MTT-S Int Microwave Symp Dig, Boston, MA (2009), 1049–1052.

© 2010 Wiley Periodicals, Inc.

SMALL-SIZE 11-BAND LTE/WWAN/WLAN INTERNAL MOBILE PHONE ANTENNA

Shu-Chuan Chen and Kin-Lu Wong

Department of Electrical Engineering National Sun Yat-sen University, Kaohsiung 80424, Taiwan; Corresponding author: wongkl@ema.ee.nsysu.edu.tw

Received 13 February 2010

ABSTRACT: This work presents an internal mobile phone antenna occupying a small board space of 600 mm² on the system circuit board and providing three wide operating bands of at least 698–960, 1710–2690, and 5150–5825 MHz for the 11-band long term evolution (LTE)/wireless wide area network (WWAN)/wideband local area network (WLAN) operation. This includes three LTE bands of LTE700/2300/2500, five WWAN bands of GSM850/900/1800/1900/UMTS, and three WLAN 2.4/5.2/5.8 GHz bands. The antenna is a coupled-fed shorted monopole, with a wide feeding strip in the coupling feed, a long shorting strip closely coupled to the shorted monopole, and a tuning stub connected to the shorting strip. The antenna's three wide operating bands are achieved and controlled by tuning the width of the feeding strip, the gap between the shorting strip and the shorted monopole, and the dimensions of the tuning stub. Operating principle of the proposed antenna is described in detail in this article. Results of the fabricated antenna are presented and discussed. The specific absorption rate results of the antenna with the presence of the user's head and hand are also studied. © 2010 Wiley Periodicals, Inc. Microwave Opt Technol Lett 52:2603–2608, 2010; View this article online at wileyonlinelibrary.com. DOI 10.1002/mop.25526

Key words: mobile antennas; handset antennas; LTE antennas; WWAN antennas; WLAN antennas

1. INTRODUCTION

To achieve small size and wideband operation is generally demanded for the internal mobile phone antennas [1]. This is a